POINT BY POINT CORRECTIONS:

General Remarks: We have reviewed the entire document based on the most recent reviewer's comment(s), with the below details. In this instance, we reviewed based on the specific corrections required by the reviewer. The specific corrections are shown in the marked up version of the manuscript also attached for your kind perusal.

Abstract Line 9: Now reads as 'The ionosphere is the major error source' instead of Ionospheric error is the major error source.'

Line 21: Now reads as 'during the equinoxes' instead 'of some months'.

Page 3 Line 52: 'posited' term have been replaced with 'posted'

Line 61: 'and affect by time' now reads as 'and is affected by time'.

Lines 61-62: 'Recently, GPS receiver is' now reads as 'Recently, dual frequency GPS receiver is'

Page 4, Line 75: 'c' is used to define the speed of light

Page 9, Line 198: The sentence now reads as 'It is well established known fact that during the day, the Sun causes'

Page 10, Line 210: 'sunrise resulting to solar EUV' now reads as 'sunrise due to solar EUV'

Page 20, line 288: 'Figure 9 show plots of the seasonal variations' now reads as 'Figure 9 show the seasonal variations'

Page 21, line 303 – 304: 'strong phenomenon in low latitudes (Aggarwal et al., 2017). The equinoctial asymmetry has been explained' have been replaced with 'strong phenomenon that occurs at low latitudes (Aggarwal et al., 2017), which has been explained'

Page 23, line 335 – 336: 'that TEC values are high' have been corrected to 'that reported higher TEC values'

Page 24, line 349 – 350: 'of TEC with solar cycle' have been replaced with 'of TEC following the solar cycle variations'

Lines 350 – 351: The text 'Our result is in good agreement with those of Chakrabarty et al. (2012) and D'ujanga et al. (2017). The former authors reported a direct solar effect on TEC while the latter authors observed that the trend in TEC follow that of solar parameters.' have been changed to 'Our result is in good agreement with those of Chakrabarty et al. (2012) and D'ujanga et al. (2017), which reported a direct solar cycle effect on TEC measurements'

Lines 353-356: In the mark up manuscript these two phrases: 'Solar activity indicates the intensity of the solar electromagnetic radiations like wavelengths of X-rays and extreme ultraviolet (EUV) radiations. These radiations vary regularly and irregularly over time, larger variability tends to occur at very short wave length.' have been deleted.

Page 25: The legend in Figure 10 now shows the monthly variations of OBS-TEC.

Line 361-362: 'and many more reported that during low' now reads as 'and many other works reported the same results during low'

Line 368: 'Balan et al. (1994) and Balan et al. (1996). Both authors in their research concluded' have been corrected to 'Balan et al. (1994, 1996), which concluded'

Page 26, Lines 372-373 in the mark up manuscript have been deleted.

Lines 373-376: The sentence 'OBS-TEC and IRI-2016 model rising from a minimum in the early hours of the day to a broad daytime maximum before falling steeply to a minimum after sunset for all years. Magnetic field tubes are rapidly filled up at dawn resulting in the increase of extreme ultraviolet (EUV) ionization (Anderson et al., 2004; D'ujanga et al., 2017).' have been changed to 'OBS-TEC and IRI-2016 model rising from a minimum in the early hours of the day to a broad daytime maximum before falling steeply to a minimum after sunset for all years, due the photoionization increase produced by the solar extreme ultraviolet radiation (Anderson et al., 2004; D'ujanga et al., 2017).'

Lines 376-377: 'OBS-TEC of many of the months were delayed till after-noon,' have been corrected to 'OBS-TEC is often delayed when compared with IRI-2016 model, with the maximum occurring afternoon,'

Lines 384-385: 'in the equinoxes and solstices as reported in the research of Fayose et al. (2012) working at Ilorin in the NEI and Eyelade et al. (2017) also working in the NEI.' is now 'in the equinoxes and solstices in the NEI as also reported by Fayose et al. (2012) and Eyelade et al. (2017).'

Lines 386-388: We now have 'September equinox' instead of 'September equinox season'

Page 27, Line 392: The sentence have been corrected to 'monthly OBS-TEC and Rz.

Line 395 – 396: 'with Rama Rao et al. (1985) that there' is now 'with Rama Rao et al. (1985) showing that there'

About reference list Malik et al 2016 have been cited in the reference list. See pages 488 – 490.

See Ayorinde et al. 2016 in lines 100, 242 in the text.

1 **DIURNAL, SEASONAL AND SOLAR CYCLE VARIATION OF TOTAL ELECTRON**

2 **CONTENT AND COMPARISON WITH IRI-2016 MODEL AT BIRNIN-KEBBI**

3 [1,*]Aghogho Ogwala, [1]Emmanuel Olufemi Somoye, [3]Olugbenga Ogunmodimu, [1]Rasaq

4 Adewemimo Adeniji-Adele, [1]Eugene Oghenakpobor Onori, [2]Oluwole Oyedokun

5 [1,*] Department of Physics, Lagos State University, Lagos, Nigeria.

6 [2] Department of Physics, University of Lagos, Nigeria.

7 [3] Department of Electrical Engineering, Manchester Metropolitan University, United Kingdom.

8 **ABSTRACT**

9 The ionosphere ~~Ionospheric error~~ is the major error source for the signals of Global Positioning

10 System (GPS) satellites. In the analysis of GPS measurements, ionospheric error is somewhat

11 assumed to be a nuisance. The error induced by the ionosphere is proportional to the number of

12 electrons along the line of sight (LOS) from the satellite to receiver and can be determined in order

13 to study the diurnal, seasonal, solar cycle and spatial variations of the ionosphere during quiet and

14 disturbed conditions. In this study, we characterize the diurnal, seasonal and solar cycle variation

15 of observed (OBS) total electron content (TEC) and compare the result with the International

16 Reference Ionosphere (IRI-2016) model. We obtained TEC from a dual frequency GPS receiver

17 located at Birnin-Kebbi Federal Polytechnic (BKFP) in Northern Nigeria (geographic location:

18 $12.64°$ N; $4.22°$ E; $2.68°$ N dip) for the period 2011 – 2014. We observed differences between the

19 diurnal variation OBS-TEC and IRI-2016 model for all hours of the day except during the post-

20 midnight hours. Slight post-noon peaks in the daytime maximum and post-sunset decrease and

21 enhancement are observed in the diurnal variation of OBS-TEC during the equinoxes ~~of some~~

22 ~~months~~. On a seasonal scale, we observed that OBS-TEC values were higher in the equinoxes than

23   the solstices only in 2012. Whereas in 2011, September equinox and December solstice recorded

24   higher magnitude followed by March equinox and lowest in June solstice. In 2013, December

25   solstice magnitude was highest, followed by the equinoxes and lowest in June solstice. In 2014,

26   March equinox and December solstice magnitude were higher than September equinox and June

27   solstice magnitude. June solstice consistently recorded the lowest values for all the years. OBS-

28   TEC is found to increase from 2011 to 2014, thus revealing solar cycle dependence.

29   **KEYWORDS:** TEC; diurnal; seasonal; variation; solar cycle 24; IRI-2016.

30   **CORRESPONDING AUTHOR PHONE:** +234 8055650264

31   **CORRESPONDING AUTHOR E-MAIL:** ogwala02@gmail.com

37

38

39

40

41

42

43

44

45

46

47

48

 1   INTRODUCTION

50   Ionospheric irregularities as a result of inhomogeneity in electron density leads to variations in the

51   intensity of radio signals (Somoye, 2010; Ogwala et al. 2018, Ogunmodimu et al. 2018). Akala et

52   al., (2011) posted ~~posited~~ that the variable nature of the equatorial/ low latitude ionosphere do

53   adversely affect communication and navigation/ satellite systems in the region. The equatorial/

54   low latitude ionosphere exhibits unique features such as the seasonal anomaly, semi-annual

55   anomaly, equinoctial anomaly, noon bite-out, spread-F, equatorial electrojet (EEJ) and equatorial

56   plasma bubbles (EPB) (Stankov, 2009; Maruyama et al., 2004; Jee et al., 2004; Codrescu et al.,

57   1999).

58   For many decades, scientists have been studying these peculiar ionospheric features and their roles

59   in trans-ionospheric electromagnetic radio wave propagation using different techniques and

60   instruments. One of the instruments often used is the GPS receiver. The GPS receiver provide

61   direct measurements from satellites. Their sounding capacity extends to the topside of the

62   ionosphere, and is affected by time and space constraints (Ciraolo and Spalla, 2002). Recently,

63   dual frequency GPS receiver is the most efficient method used to eliminate the effect of the

64   ionosphere on radio signals. This method combine signals in different L band frequencies, L1

65   (1575 MHz) and L2 (1228 MHz) (Bolaji et al., (2012; Alizadeh et al., 2013).

66   Almost all space geodetic techniques transmit signals in at least two different frequencies

67   for better accuracy (Alizadeh et al., 2013). The signals are then combined linearly in order to

68   eliminate the effect of the ionosphere on radio signals. The ionospheric effect on radio signal is

69   proportional to the total electron content (TEC), which is defined as the number of electrons per

70   square meter from satellite in space to receiver on ground as shown in Eq. (1).

71    $TEC = \int n_e(s)ds$ $\hspace{8cm}$ (1)

72   It is measured in multiples of TEC units (1 TECU = 10^{16} el/m^2). Due to the dispersive nature of

73   the ionosphere, there is a time delay between the two frequencies of a GNSS signal as it propagate

74   through the ionosphere as shown in Eq. (2) as $\Delta t = t_2 - t_1$. Thus,

75    $$\Delta t = \left(\frac{40.3}{c}\right) \times \frac{TEC}{\left[\left(\frac{1}{f_2^2}\right)-\left(\frac{1}{f_1^2}\right)\right]} \qquad (2)$$

76   Where ~~C~~ c is speed of light and f is frequency. Hence, Δt measured between the L1 and L2

77   frequencies is used to evaluate TEC along the ray path.

78   When Global Navigation Satellite System (GNSS) signals propagate through the ionosphere, the

79   carrier experiences phase advance and the code experiences a group delay due to the electron

80   density along the line of sight (LOS) from the satellite to the receiver (Bagiya et al., 2009; Tariku,

81   2015). Thus, the carrier phase pseudo ranges are measured too short, and the code pseudo ranges

82   are measured too long compared to the geometric range between the satellite and the receiver. This

83   results in a range error of the positioning accuracy provided by a GPS receiver. The range error

84   due to TEC in the ionosphere varies from hundreds of meters at mid-day, during high solar activity

85   when the satellite is near the horizon of the observer, to a few meters at night during low solar

86   activity, with the satellite positioned at zenith angle (Bagiya et al., 2009). By measuring this delay

87   using dual frequency GPS receivers, properties of the ionosphere can be inferred and used to

88   monitor space weather events such as GNSS, HF communications, Space Based Observation

89   Radar and Situational Awareness Radar, etc. Ionospheric delay (proportional to TEC) is the highest

90   contributor to GPS positioning error (Alizadeh et al., 2013; Bolaji et al., (2012).

91   TEC in the ionosphere can also be studied using empirical ionospheric model such as the

92   International Reference Ionosphere (IRI). IRI is a joint undertaking by the Committee on Space

93   Research (COSPAR) and International Union of Radio Science (URSI) with the goal of developing

94 and improving an international standard for the parameters in earth's ionosphere (Bilitza et al.,

95 2014). An updated version has been recently developed to cater for lapses of previous models. IRI

96 provides the vertical TEC (VTEC) from the lower boundary (60 – 80 km) to a user-specific upper

97 boundary (Bilitza et al., 2016).

98   In the past few decades, studies on the temporal and spatial variations of TEC have gained

99 popularity in the scientific community (Wu et al., 2008). However, understanding the variability

100 of TEC will also go a long way in obtaining the positioning accuracy of GNSS under disturbed

101 and quiet conditions. As such, previous studies (e.g. Ayorinde et al., 2016; Bhuyan and Borah,

102 2007; Maruyama et al., 2004; Jee et al., 2004; Balan et al., 1994; Rama Rao et al., 2006a, b, c;

103 Rama Rao et al., 1985; Bolaji et al. 2012; Wanninger, 1993; Akala et al., 2013; Komjathy et al.,

104 1998; Langley et al., 2002 Sunda et al., 2013; Torr and Torr, 1973; Tsai et al., 2001 and references

105 therein) investigated the global distribution of TEC variations and its characteristics at all latitudes,

106 during different solar cycle phases under disturbed and quiet conditions.

107   Studies of Rama Rao et al. (2006a, b) in the Indian sector and Wanninger (1993) in the

108 Asian sector reported maximum day-to-day variability in TEC at the Equatorial Ionization

109 Anomaly (EIA) crest regions, increasing peak value of TEC with increase in integrated equatorial

110 electrojet (IEEJ) strength, maximum monthly average diurnal variations during equinox months

111 followed by winter months and lowest during summer months. They also reported positive

112 correlation of TEC and EEJ and the spatial variation of TEC in the equatorial region. Titheridge

113 (1974) and Langley et al. (2002) attributed the lowest TEC values during the summer seasons to

114 low ionization density resulting from reduced O/N_2 ratio (production rates) as a result of increased

115 scale height. Bhuyan and Borah (2007) working in the Indian sector and Komjathy et al. (1998)

116 and Lee and Reinisch (2006) while studying in the American sector compared TEC derived from

GPS receivers with IRI model in the equatorial/ low latitude sector and inferred that the diurnal amplitude of TEC is higher during the equinoxes followed by December solstices and lowest in June solstice, i.e., observing winter anomaly in seasonal variation. They further reported discrepancies between IRI model and their measured values during most hours of the day at their various locations. Malik et al. (2016) on their studies over the Malaysian peninsular reported higher IRI values than observed maximum useable frequency (MUF) values but behaves similarly diurnally and seasonally with no clear trend. Akala et al. (2013) on the comparison of equatorial GPS-TEC observations over an African station and an American station during the minimum and ascending phases of solar cycle 24 reported that seasonal VTEC values were maximum and minimum during March equinox and June solstice respectively, during minimum solar cycle phase at both stations. They also reported that during the ascending phase of solar cycle 24, minimum and maximum seasonal VTEC values were recorded during December solstice and June solstice respectively. They further showed that IRI-2007 model predicted better in the American sector than the African sector.

The aim of this paper is (i) to characterize TEC on diurnal, seasonal and solar cycle scales in the Nigerian Equatorial ionosphere (ii) to compare OBS-TEC with IRI-2016 model in order to find if the model underestimates or overestimates TEC values at the African longitudinal sectors. In section 2, we describe the data and methodology. Section 3 shows the result and discussion while concluding remarks are in section 4.

2   DATA AND METHODOLOGY

2.1   DATA

The Receiver Independence Exchange (RINEX) Observation GPS data files were downloaded daily from NIGNET website (www.nignet.net) and processed using Bernese software

140 and GPS TEC analysis software. The RINEX file contains 60 iteration data (i.e. in 1 minute time

141 resolution). The GPS-TEC analysis software was designed by Gopi Seemala of the Indian Institute

142 of Geomagnetism. The summary of this application is to read raw data, processes cycle slips in

143 phase data, reads satellite biases from the International GNSS services (IGS) code files (and

144 calculates them if unavailable), and calculates receiver bias, inter-channel biases for different

145 satellites in the constellation, and finally plots the VTEC values on the screen and writes the ASCII

146 output files (*CMN) for STEC and (*STD) for VTEC in the same directory of the data files. Effect

147 due to multipath is eliminated by using a minimum elevation angle of 50°.

148   Observation GPS-TEC obtained from the TEC analysis software is the slant TEC (STEC)

149 and vertical TEC (VTEC). STEC is polluted with several biases that must be eliminated to get

150 VTEC. VTEC is calculated from the daily values of STEC using Eq. (3).

151 $VTEC = (STEC - [b_R + b_S + b_{RX}])/S(E)$ (3)

152 Where b_R, b_S, and b_{RX} are receiver bias, satellite bias and receiver interchannel bias respectively.

153 S(E), which is the oblique factor with zenith angle, z at IPP (Ionospheric Pierce Point) is expressed

154 in Eq. (4).

155 $S(E) = \frac{1}{\cos(z)} = \left\{ 1 - \left(\frac{R_E \times \cos(E)}{R_E + h_S} \right)^2 \right\}^{-0.5}$ Bolaji et al. (2012)   (4)

156 R_E = the mean radius of the earth in km and h_S = ionospheric height from the surface of the earth.

157 According to Rama Rao et al., (2006c), ionospheric shell height of approximately 350km is

158 appropriate for the equatorial/ low latitude region of the ionosphere for elevation cut off angle of

159 > 50°. This is valid in this study.

160   Hourly VTEC data obtained from these processing software are averaged to daily TEC

161 values in TEC units (1 TECU = 10^{16} el/m^2). OBS-TEC from Birnin-kebbi, on geographic Latitude

162 12.47° N and geographic Longitude 4.23° E located in Northern Nigeria, obtained during the

163 period 2011 – 2014, which corresponds to the ascending (2011 – 2013) and maximum (2014)

164 phases of solar cycle 24 were compared with derived TEC obtained from International Reference

165 Ionosphere (IRI-2016) model website

166 (https://ccmc.gsfc.nasa.gov/modelweb/models/iri2016_vitmo.php). The 2016 version of IRI

167 provides important changes and improvements on previous IRI versions (Bilitza et al., 2016). Solar

168 cycle 24 is regarded as a quiet solar cycle which peaked in 2014 with maximum sunspot number

169 (103) occurring in February. Values of sunspot number, Rz, in Text format were obtained from

170 Space Physics Interactive Data Resource (SPIDR) website (www.ionosonde.spidr.com) shortly

171 before it became unavailable. Table 1 shows the years used in this study and their corresponding

172 sunspot number, Rz.

173

174 Table I: Table of years, solar cycle phase and sunspot number, Rz [Source: Author].

Years	Solar Cycle Phase	Sunspot Number, R_z
2011	Ascending	55.7
2012	Ascending	57.6
2013	Ascending	64.7
2014	Maximum	79.6

175

176 **2.2   METHODOLOGY**

177 Diurnal variations of hourly OBS-TEC and hourly IRI-2016 model (NeQuick topside

178 option) were plotted using the monthly mean values of OBS-TEC and monthly mean of IRI-2016

179 model against local time (LT) on the same Figure. The corresponding percentage deviation

180 (percentage Dev or % DEV) of IRI-2016 from OBS-TEC were also analysed using the monthly

181   mean values of OBS-TEC and monthly mean values of IRI-2016 against local time (LT).

182   Percentage Dev is obtained using Eq. (5) below:

183    $$\%DEV = \left(\frac{OBS-IRI}{OBS}\right) \times 100 \qquad\qquad (5)$$

184   where OBS represents Observation-TEC values and IRI represents TEC derived by IRI-2016

185   model.

186   The OBS-TEC data was grouped following Onwumechilli and Ogbuehi (1964) into four

187   seasons namely: March equinox (February, March and April), June solstice (May, June and July),

188   September equinox (August, September and October) and December solstice (November,

189   December and January), in order to investigate seasonal variation. Finally, Annual variation of

190   OBS-TEC and sunspot number, Rz were also analysed by plotting mean OBS-TEC and mean Rz

191   against each month of the year.

192   **3   RESULT AND DISCUSSIONS**

193   Figures 1 to 4 show the diurnal variation of OBS-TEC and IRI-2016 model in the Nigerian

194   Equatorial Ionosphere (NEI) for the years 2011 to 2014 respectively. OBS-TEC were obtained

195   from the GPS receiver installed at Birnin-Kebbi station. The diurnal variation of OBS-TEC and

196   IRI-2016 model TEC reveals the typical characteristics of an equatorial/ low latitude ionosphere.

197   We show the day-to-day variation of OBS-TEC with error bar showing the standard deviation from

198   mean values. The study reveals that day-to-day variation of OBS-TEC is higher during the daytime

199   than night time for all the years. It well established known fact that during the day, the sun causes

200   variations in temperature, neutral wind, electron density and electric field thereby modulating the

201   structure and evolution of the ionosphere and thermosphere (Gorney, 1990; Forbes et al. (2006).

202   These Figs. show a steep rise in OBS-TEC from a minimum of ~2 TECU between 03:00 – 05:00

203   LT in 2011, ~3 TECU (04:00 – 05 LT) in 2012, ~3 TECU (03:00 – 05:00 LT) in 2013 and 2014.

204 OBS-TEC increased to a broad daytime maximum between 12:00 LT – 14:00 LT for all years

205 before falling to a minimum after sunset. The diurnal variation of IRI-2016 model shows TEC

206 increasing from a minimum of ~ 2 TECU in 2011, ~ 4 TECU in 2012 and 2013, and ~ 5 TECU in

207 2014 between 03:00 – 04:00 LT for all years, to a broad daytime peak between 08:00 – 14:00 LT,

208 before falling steeply to minimum before sunset. Hence the IRI-2016 model attained its peak

209 before OBS-TEC. Dabas et al. (2003); Somoye et al. (2011); Hajra et al. (2016); D'ujanga et al.

210 (2017) attributed the steep increase in TEC to the upward $\mathbf{E} \times \mathbf{B}$ vertical plasma drift and the rapid

211 filling up of the magnetic field tube at sunrise due ~~resulting~~ to solar EUV ionization. During

212 daytime, an eastward electric field at the equator causes plasma to be lifted to greater heights. This

213 dynamo-generated eastward electric field combined with the northward geomagnetic field lifts the

214 equatorial ionosphere from 700 km to 1000 km, resulting in additional ionization (D'ujanga et al.,

215 2017; Somoye et al., 2011). Suranya et al., 2015 further mentioned that upward vertical $\mathbf{E} \times \mathbf{B}$ drift

216 could lead to equatorial ionization anomaly (EIA) and meridional winds. The magnetic field tubes

217 then collapse after sunset due to low thermospheric temperature and Rayleigh Taylor Instability

218 (RTI) (Berkner and Wells, 1934) giving rise to the minimum TEC values after sunset. These results

219 are similar to findings of Bolaji et al., (2012), Fayose et al., (2012), Okoh et al., (2014), Eyelade

220 et al., (2017) who have explored the NEI.
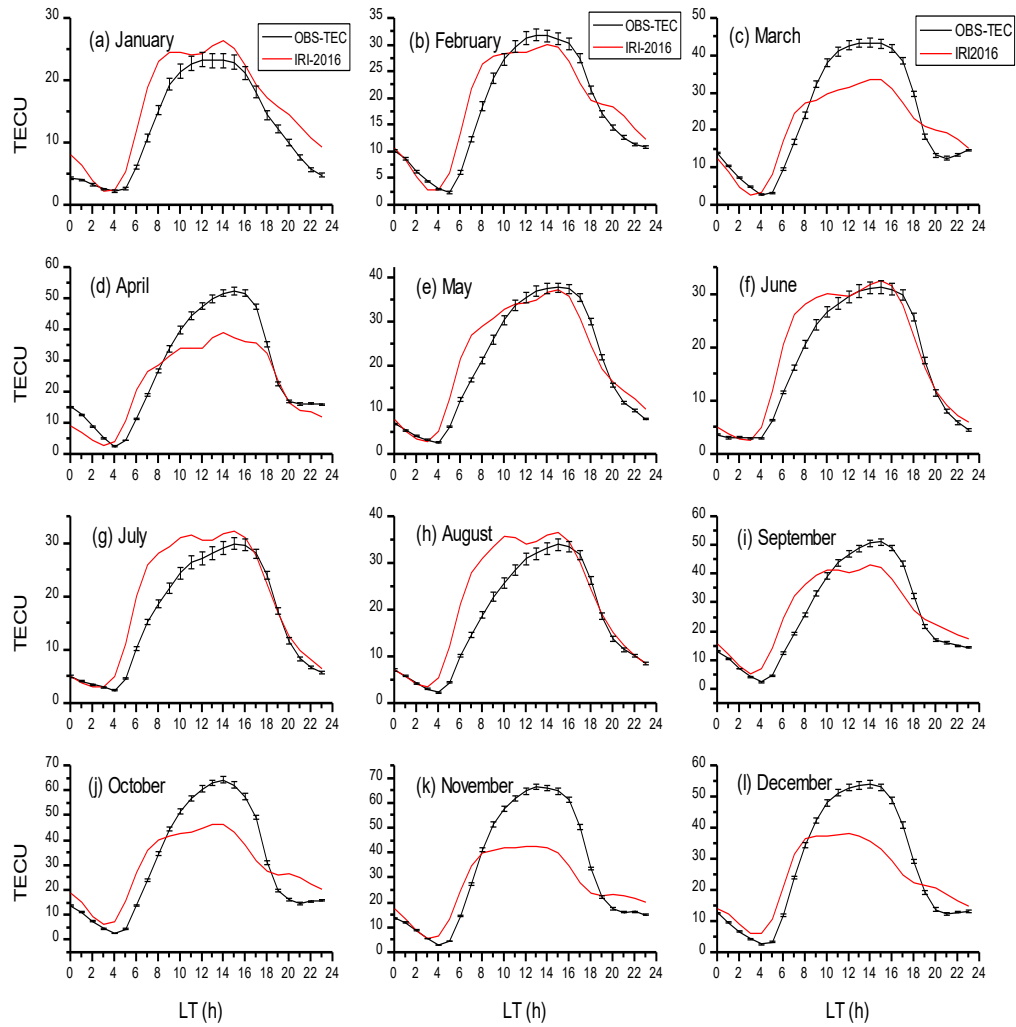
221   Fig. 1: Diurnal variation of OBS-TEC showing error bar and IRI-2016 model of each month during
       January – December 2011 at Birnin-Kebbi
222
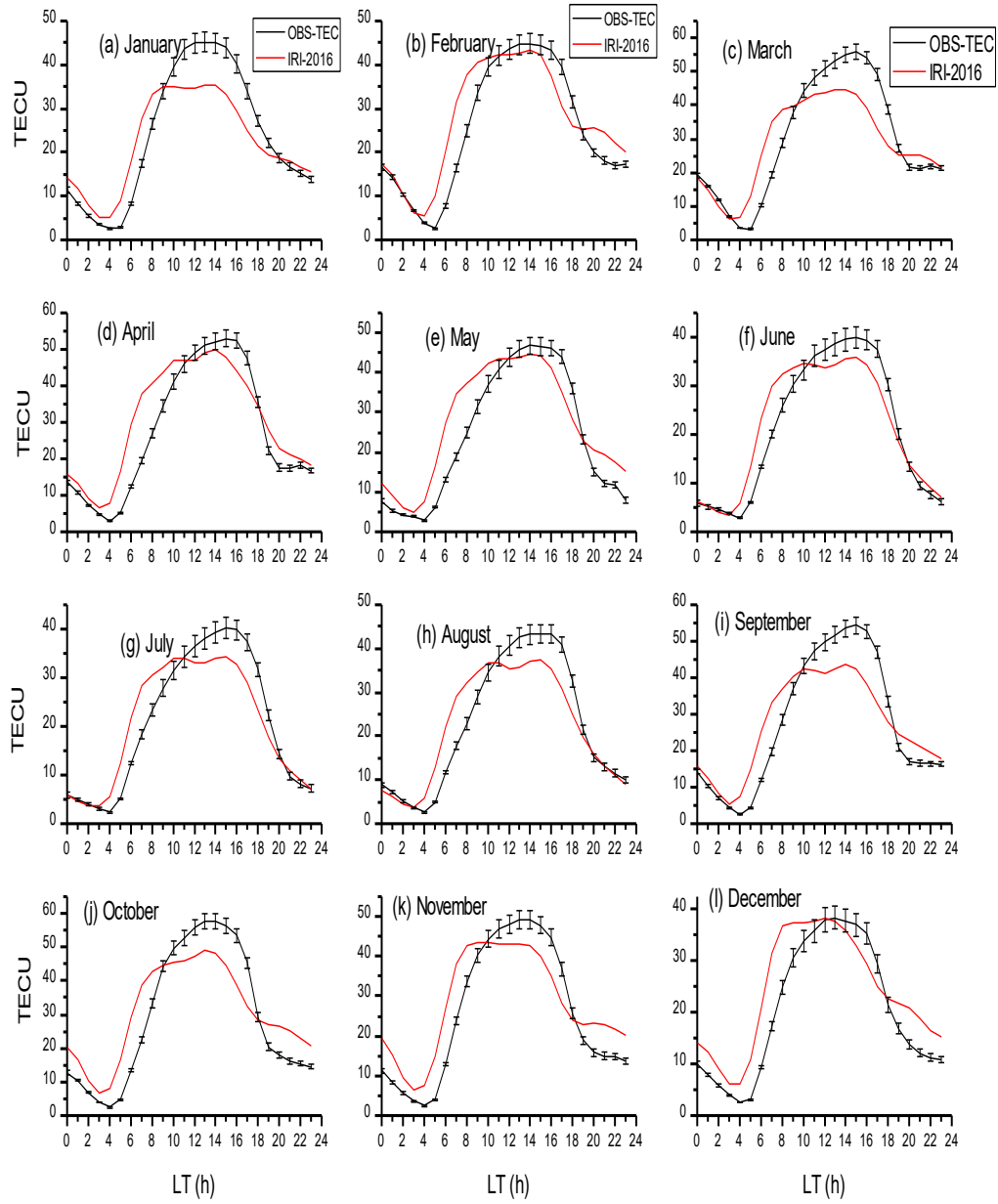
Fig. 2: Same as Figure 1 for 2012.

223

224

225

226
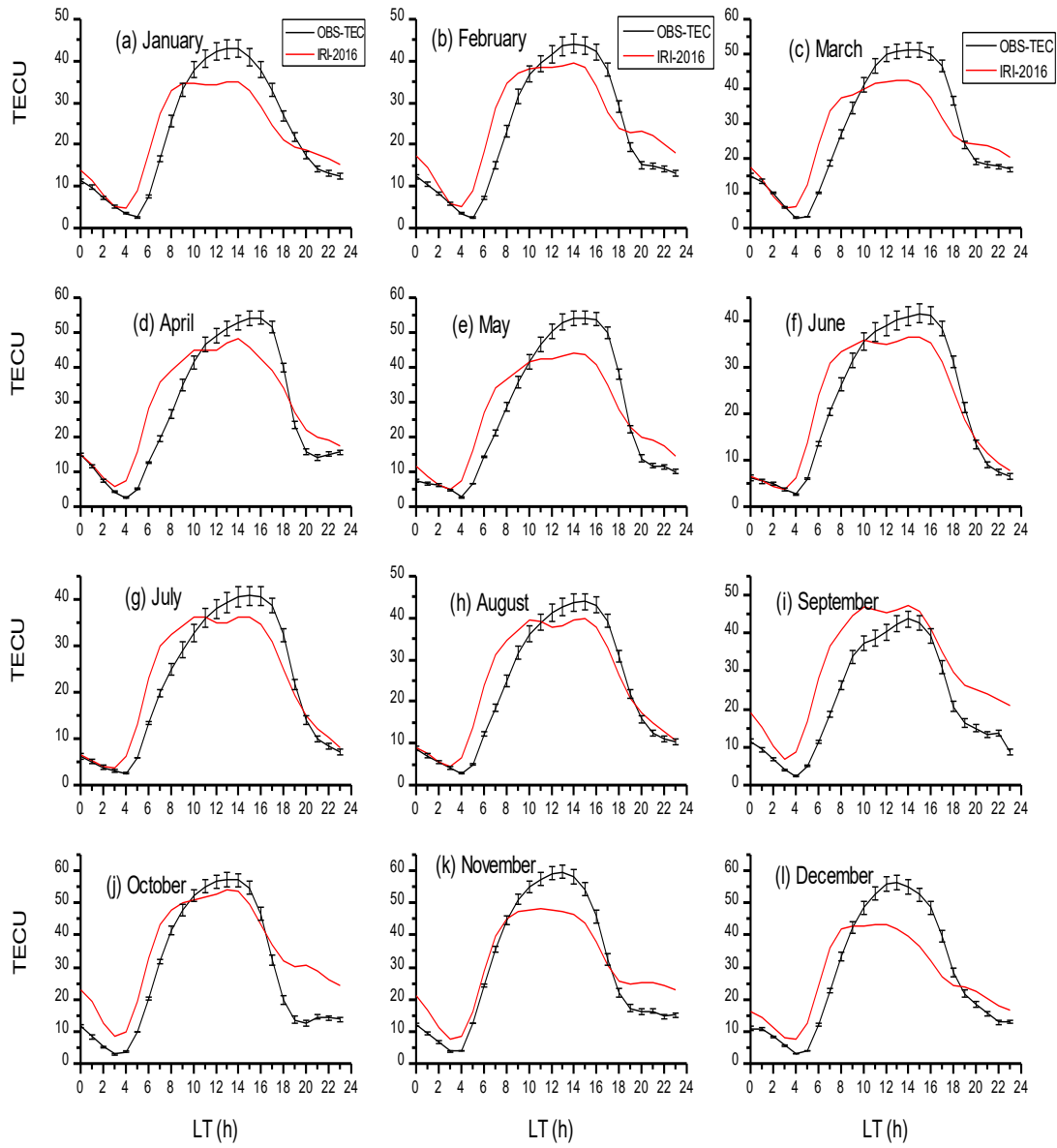
Fig. 3: Same as Figure 1 for 2013.

227

228

229

230
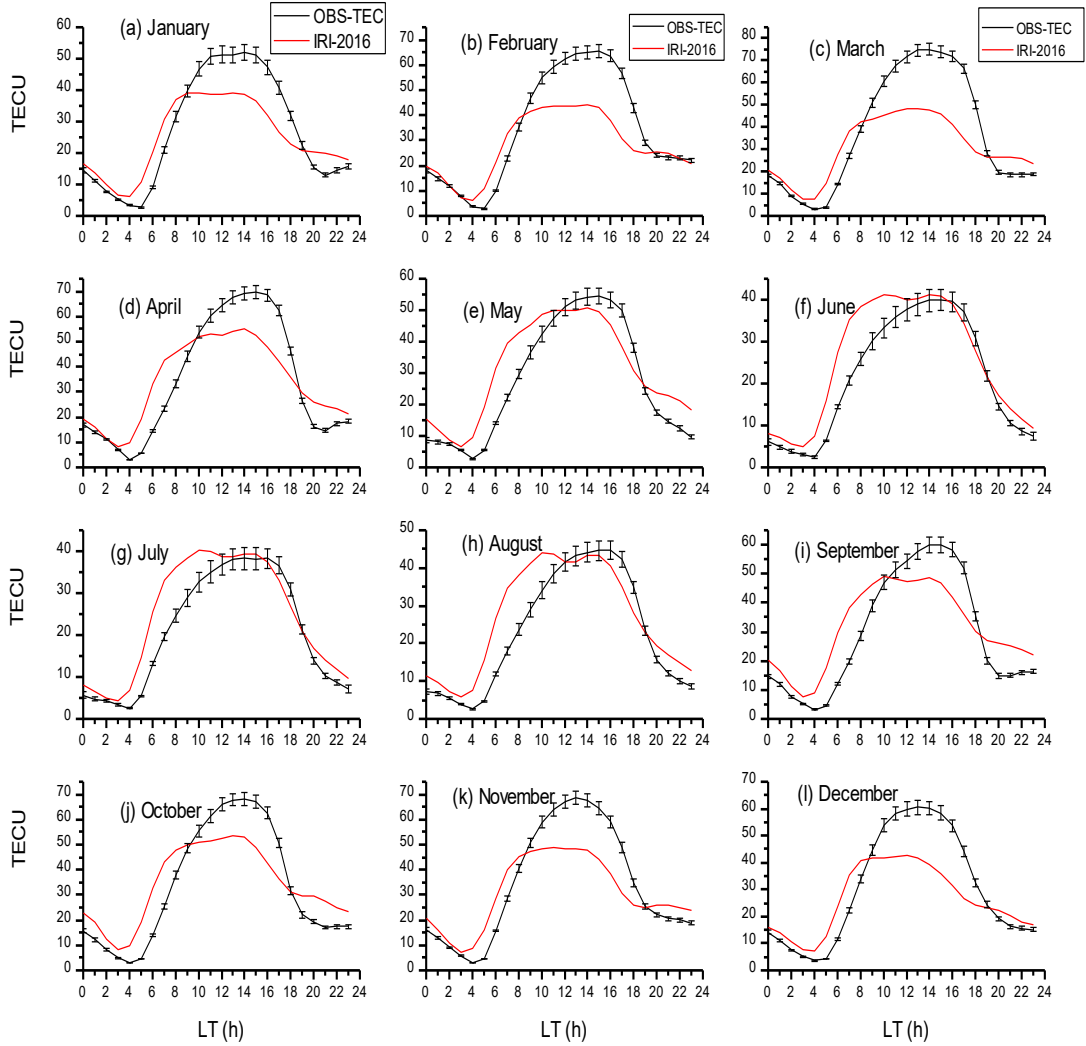
Fig. 4: Same as Figure 1 for 2014.

231

232   It can be seen that OBS-TEC is much higher in 2014 with maximum value up to 70 TECU

233   in March compared with IRI-2016 maximum of 54 TECU in the month of October, 2014. The

234   diurnal variation reveals that the peak of OBS-TEC of majority of the months for all years shifted

235   to slightly post-noon hours (13:00 – 14:00 LT). This type of peak shifting is peculiar to equatorial/

236   low latitude regions and the Polar Regions of the ionosphere and it is found to depend on the

237   equatorial ionization anomaly and solar zenith angle respectively (Rama Rao et al., 2009; D'ujanga

238 et al., 2017). Another key observation seen in the diurnal variation of OBS-TEC is the post-sunset

239 decrease and slight enhancement in some months. The night time enhancement of TEC, for

240 example, March, April and October of the year 2011, March and April of the year 2012, March,

241 April, September and October of the year 2013, January, April and September of the year 2014

242 was documented by previous researchers like Rama Rao et al., 2009; D'ujanga et al., 2017 and

243 Ayorinde et al., 2016. They attributed it to the product of eastward and westward directed electric

244 field which produces an upward and downward motion of ionospheric plasma during the day and

245 night respectively.

246   Figures 5 to 8 show the diurnal variation of percentage deviation of IRI-2016 model from

247 OBS-TEC in the Nigerian Equatorial Ionosphere (NEI) for all years respectively. On a general

248 note, IRI-2016 model only presented suitable predictions for the post-midnight hour between 00 –

249 03 LT of the day for all years. All other hours from 04 – 23 LT show some discrepancies. In fact,

250 for some of the months: October, November and December of 2012, October and December, 2013,

251 and September and October of 2014, these discrepancies lasted throughout the day. Whereas in

252 some other months: June, July and August of 2011, June, July and August of 2012, June and

253 August of 2013 and February, June and July of 2014, these discrepancies collapsed during the pre-

254 midnight hours (18 – 23 h). It is also important to mention that IRI-2016 model either over

255 estimated or under estimated TEC in the NEI especially during daytime hours as shown in the

256 plots.

257

258

259

260
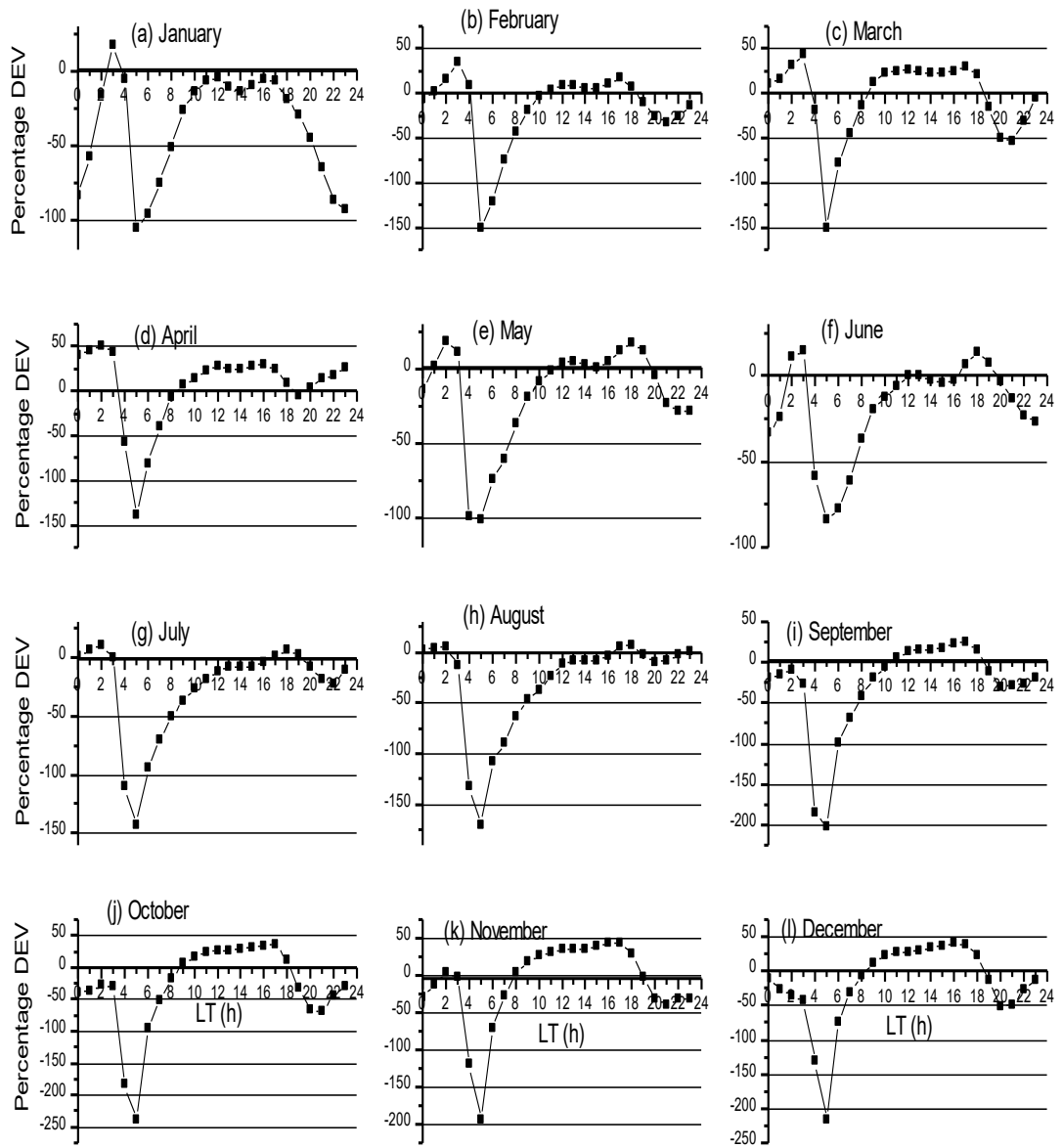
Fig. 5: Percentage deviation of IRI-2016 from OBS-TEC for year 2011

261

262

263
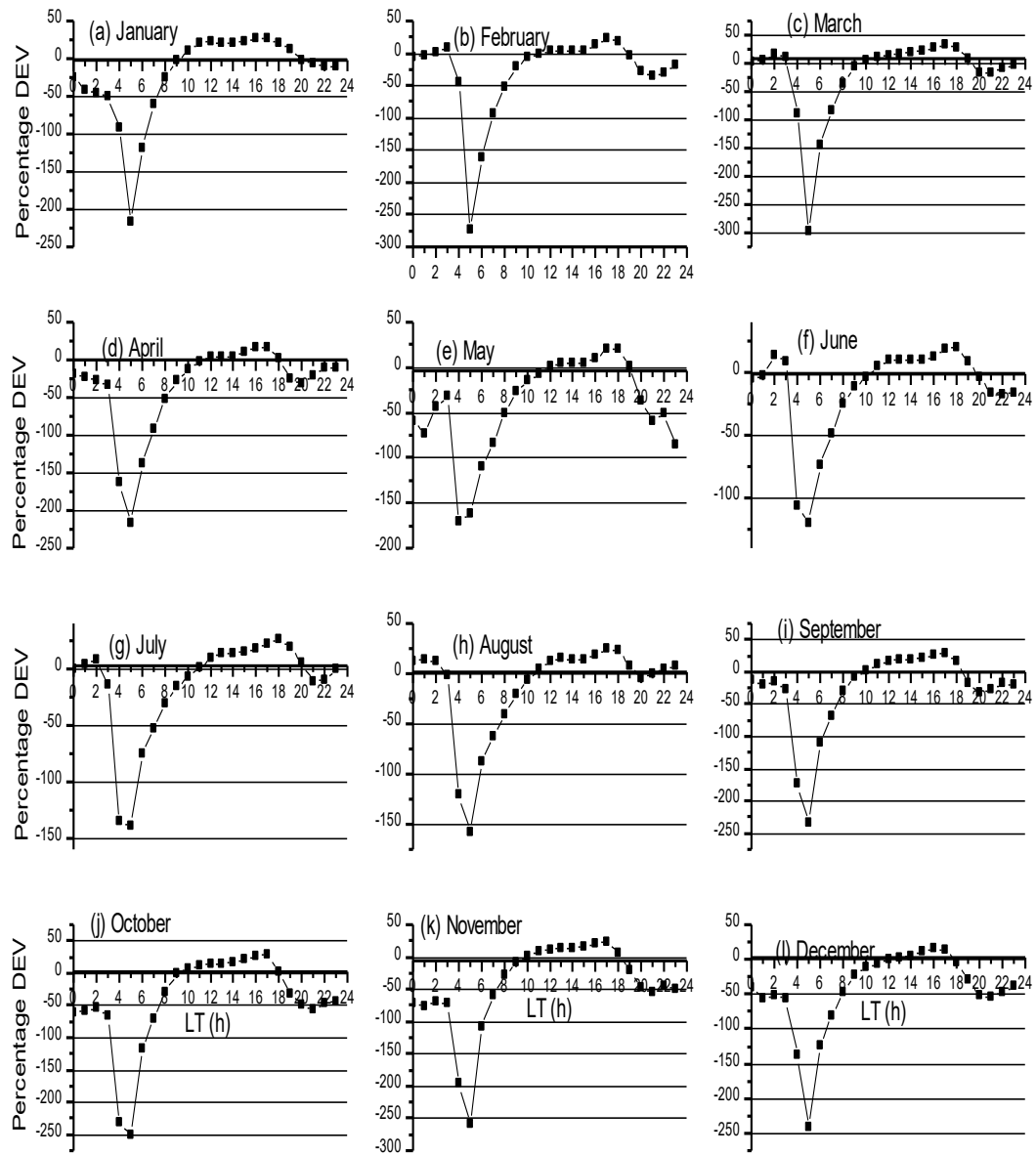
Fig. 6: Percentage deviation of IRI-2016 from OBS-TEC for year 2012

264

265

266
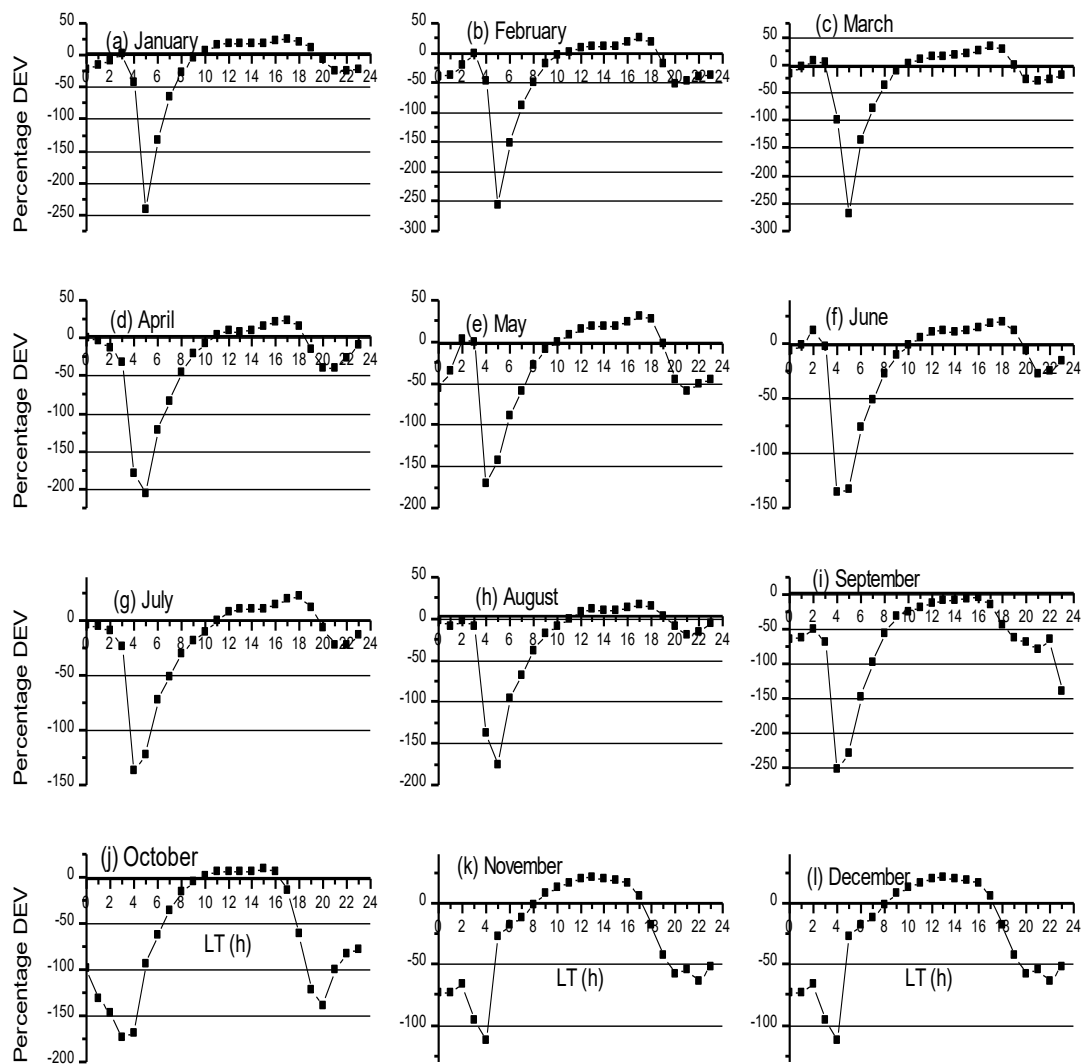
Fig. 7: Percentage deviation of IRI-2016 from OBS-TEC for year 2013

267

268

269

270

271
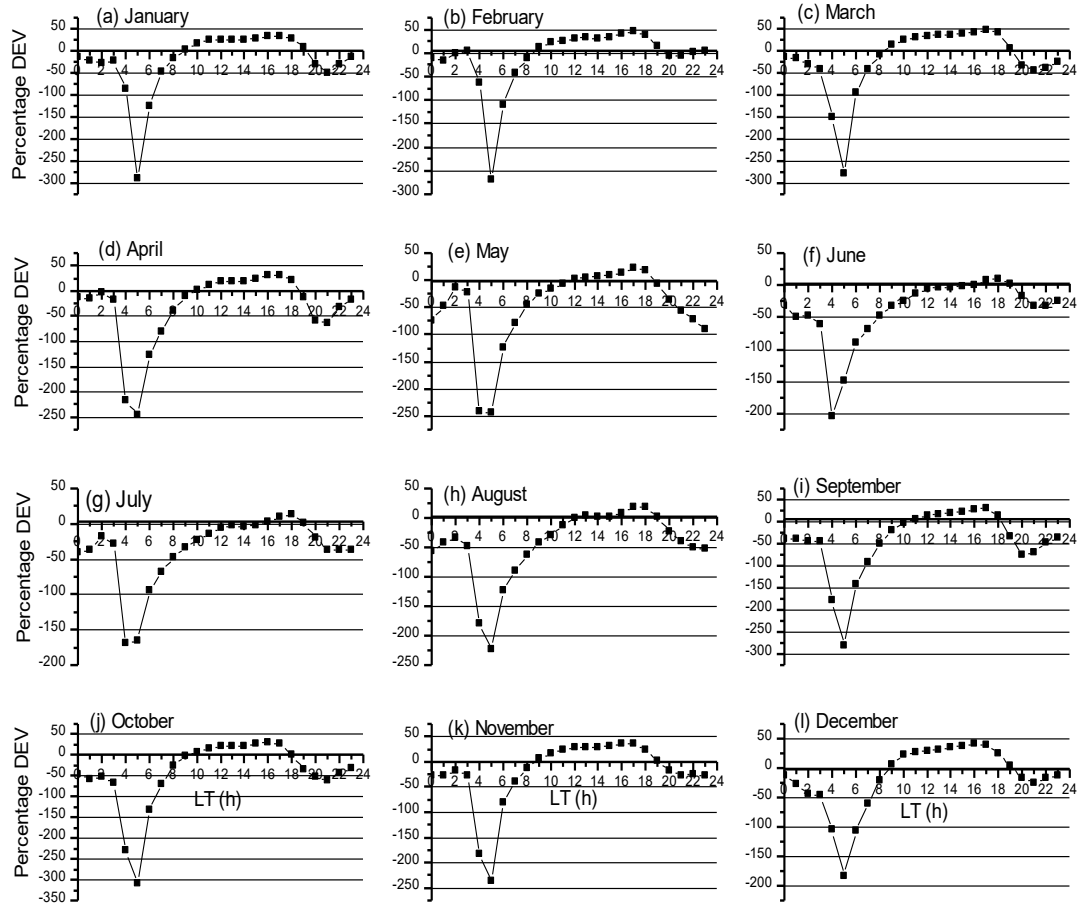
Fig. 8: Percentage deviation of IRI-2016 from OBS-TEC for year 2014

272

273   The mass plots in Fig. 5 – 8 further reveal that negative percentage deviation shows higher

274   values of IRI-2016 than OBS-TEC values. The reverse is the case for positive percentage

275   deviation. Highest negative percentage deviations are seen between 04 – 05 LT for all months

276   throughout the years in this study. Highest Negative percentage deviation of ~ 300% was recorded

277   in the month of October, 2014 at 05 LT. Table II shows the summary of months with daytime

278   over- or under-estimate of IRI-2016 in the NEI.

279

280   Table II: Months of daytime estimate of IRI-2016 model in NEI [Source: Author]

YEAR	OVER ESTIMATE	UNDER ESTIMATE	SAME RANGE
2011	January, July, August	February – April, September - December	May - June
2012		January - December	
2013	September	January – August, October - December	
2014		January - December	

281

282   Therefore, it is clear from Fig. 1- 4, Fig. 5 – 8 and Table II that IRI-2016 model did not

283 predict well in the NEI. This may be attributed to insufficient data which is as a result of the sparse

284 distribution of GPS infrastructure in this region. Our result agree with those Komjathy et al. (1998);

285 Lee and Reinisch (2006); Malik et al. (2016). Bhuyan and Borah (2007) reported higher IRI TEC

286 than their measured values at about all local time in their location. Mosert et al. (2007) and Sethi

287 et al. (2010) also reported discrepancies between of IRI TEC predictions and GPS TEC during

288 high solar activity (HSA) and low solar activity (LSA) respectively at equatorial/ low latitudes.

289   Figure 9 show ~~plots of~~ the seasonal variations of OBS-TEC for the four years investigated.

290 The change in concentration of Oxygen and molecular Nitrogen has been reported to be the main

291 cause of seasonal variation of ionospheric parameters. Seasonal variation of OBS-TEC in this

292 study depicts semi-annual variation with equinoctial maximum (~ 52 TECU) and solsticial

293 minimum (~ 44 TECU) in 2012. D'ujanga et al., (2017) reported that since the sun passes through

294 the equator during the equinox, both March and September equinox experience the same solar

295 radiation. It is also a well-established fact that March 20 and September 23 are the only times in

the year when the solar terminator is perpendicular to the equator, giving rise to the equinoctial maximum. The semi-annual variation resulting from the effect of equatorial ionization anomaly (EIA) in the ionosphere has been attributed to the effect of solar zenith angle and magnetic field geometry (Wu et al., 2008; Rama Rao et al., 2006a). Another important feature of ionospheric parameters (known as equinoctial asymmetry) which is reported in the work of Bolaji et al., (2012); Akala et al., (2013); Eyelade et al., (2017); D'ujanga et al., (2017); Aggarwal et al., (2017), is clearly seen in all years used in this work. Akala et al., (2013) also reported minimum and maximum seasonal VTEC values during June solstice and December solstice respectively, during ascending phase of solar cycle 24. Equinoctial asymmetry is a strong phenomenon that occurs at in low latitudes (Aggarwal et al., 2017), which . The equinoctial asymmetry has been explained in terms of the differences in the meridional winds leading to changes in the neutral gas composition during the equinoxes.

311
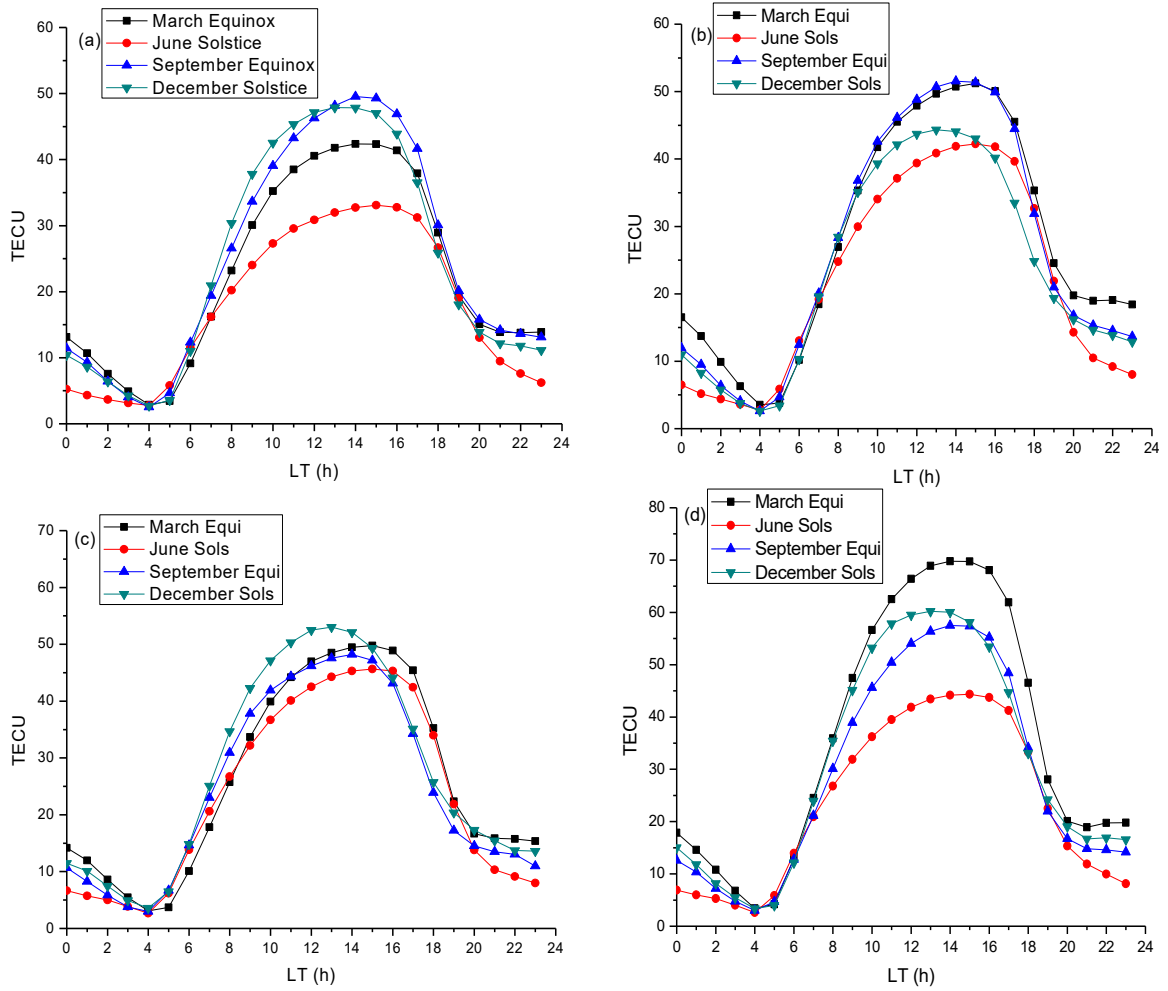
Fig. 9: Seasonal variation of observed OBS-TEC during (a) 2011 (b) 2012 (c) 2013 and (d)
312   2014

313   In 2011, September equinox and December solstice recorded higher magnitude, followed

314 by March equinox; the lowest was in June solstice. In 2013, December solstice magnitude was

315 highest, followed by the equinoxes, March and September respectively and lowest in June solstice.

316 This corresponds to result obtained by Akala et al. (2013), which they attributed to increase in ion

317 production rate in winter season and anti-correlation between December and June Solstice pre-

318 reversal velocity enhancement. In 2014, March equinox magnitude was highest, December solstice

319 and September equinox magnitudes were about same range while June solstice magnitudes were

least. December solstice magnitude is found to occur between the magnitudes of the equinoxes in 2011 and 2014. The September equinox magnitude and March equinox magnitude are observed to interchange in 2011 and 2014. Overall, June solstice magnitudes were lowest during all the years. Titheridge (1974) attributed the June solstice least magnitudes to low ionization resulting from reduced production rates, i.e. O/ N_2 ratio.

Also, for all seasons, pre-midnight (18 – 23 LT) values of TEC are higher than post-midnight (00 – 05 LT) TEC values for all years. In 2011, pre- midnight TEC values are in the range of 8 – 30 TECU while post-midnight TEC values ranges from 3 to 13 TECU. In 2012, pre-midnight TEC values are in the range of 9 – 35 TECU while post-midnight TEC values are between 3 to 17 TECU. In 2013, the pre-midnight TEC values are between 9 – 35 TECU while post-midnight TEC values ranges from 3 – 15 TECU. Finally in 2014, pre-midnight TEC values are between 9 to 47 TECU while the post-midnight TEC ranges from 3 to 18 TECU. Furthermore, the maximum OBS-TEC values in 2011 (49 TECU) and 2012 (52 TECU) were recorded in September Equinox season. In 2013, OBS-TEC reached a maximum of 53 TECU in December solstice while in 2014, the maximum OBS-TEC (70 TECU) was recorded in March Equinox season in the NEI (West African sector). This result agrees in general with those of D'ujanga et al. (2017) who obtained higher TEC values during the equinoxes than during the solstices in Ethiopia (East African sector). This same result was observed by Bagiya et al. (2009) that reported higher TEC values that TEC values are high in equinoctial months than solsticial months in the Indian sector. While the former authors reported maximum TEC of ~ 58 TECU during the equinox months, the latter authors reported maximum TEC ~ 50 TECU during the equinoxes. Seasonal variation of TEC is dependent on thermospheric neutral compositions since during the day the equator is hotter than the pole. Meridional winds therefore flows from the equator towards the pole. This flow cause

343   a change in the neutral composition resulting in the decrease of the ratio of O/N_2 at the equator.

344   The decrease of O/N_2 ratio increases the electron density, and thus resulting in TEC increase

345   during the equinoxes (Bagiya et al., 2009). The corresponding annual range error (meters) of the

346   season with maximum OBS-TEC using 1 TECU variation to represent an error of 0.16 m in

347   position is summarized in Tables III.

348   Table III: Season of maximum OBS-TEC and their corresponding range error.

YEAR	SEASON OF MAXIMUM OBS-TEC	VALUE (TECU)	CORRESPONDING ERROR (m)
2011	September Equinox	49	8
2012	September Equinox	52	8
2013	December Solstice	53	8
2014	March Equinox	70	11

349

350   Figure 10 shows the comparison of the monthly mean OBS-TEC and monthly mean

351   sunspot number, Rz from 2011 – 2014, showing an increase and decrease of TEC following the

352   ~~with~~ solar cycle variations. Our result is in good agreement with those of Chakrabarty et al. (2012)

353   and D'ujanga et al. (2017), which reported a direct solar cycle effect on TEC measurements. ~~The~~

354   ~~former authors reported a direct solar effect on TEC while the latter authors observed that the trend~~

355   ~~in TEC follow that of solar parameters.~~ Solar cycle dependency of ionospheric parameters such as

356   TEC provides useful information to study the behavior and variations of the physical and

357   photochemical processes in the ionosphere (Liu et al. 2006). ~~Solar activity indicates the intensity~~

358   ~~of the solar electromagnetic radiations like wavelengths of X-rays and extreme ultraviolet (EUV)~~

359   ~~radiations. These radiations vary regularly and irregularly over time, larger variability tends to~~

360 ~~occur at very short wave length.~~ It is well documented that the variability of solar activity results

361 in huge variations in the temperature, neutral wind, neutral density, ion and electron densities and

362 electric fields in the ionosphere (Forbes et al. 2006).

363

364
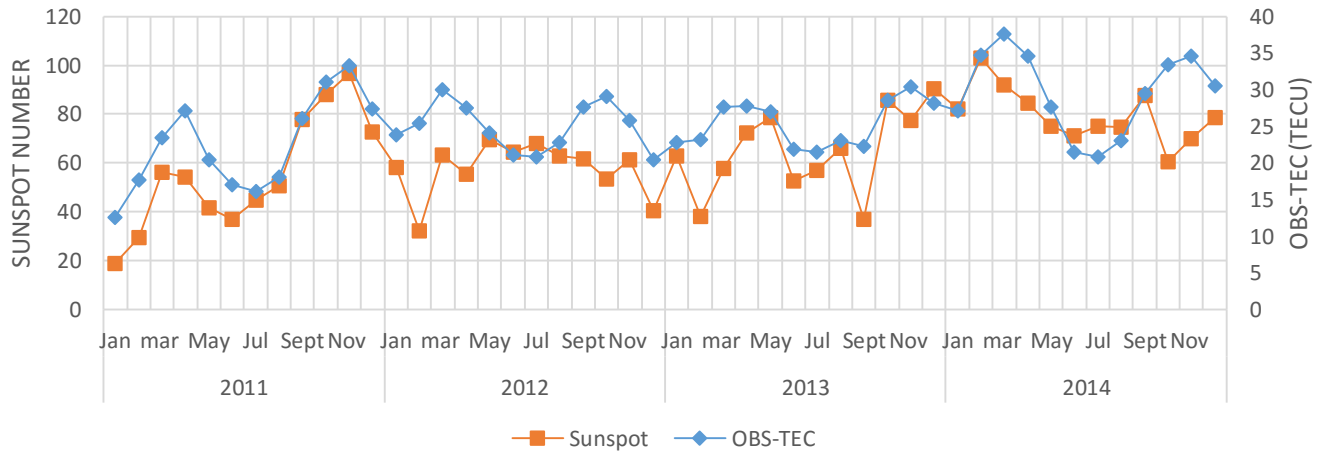
Figure 10: ~~Annual~~ Monthly variation of OBS-TEC with sunspot number, Rz at Birnin-Kebbi

365

366 The present result also agrees with that of Rama Rao et al. (1985) who reported a direct

367 solar control on TEC. Balan et al. (1994); Liu et al. (2011) and Liu et al. (2006) and many other

368 works ~~more~~ reported the same results ~~that~~ during low and moderate solar activity, TEC and N_mF_2

369 increases linearly with solar proxies, but the linearity collapse during high solar activity. This

370 agrees with our result except for July month of 2012 and 2014 which shows saturation effect on

371 TEC i.e decrease in TEC with increase in solar activity. The saturation effect on TEC was reported

372 in the work of Balan et al. (1994, 1996), which ~~and Balan et al. (1996). Both authors in their~~

373 ~~research~~ concluded that the saturation effect has not been clarified and hence might be due to other

374 factors near the earth's environment and not as a result of the influence of solar activity. We could

375 not establish the cause of the saturation effect on TEC in this study, however, saturation effect will

376 be further investigated in future studies. ~~Ionospheric climatology especially solar activity and the~~

377 ~~equatorial ionization anomaly (EIA) effects of the `ionosphere provides an insight into space~~

378 ~~weather events (Liu et al., 2011).~~

379 **4   CONCLUSIONS**

380 Studies on OBS-TEC and IRI-2016 model at Birnin-Kebbi in Northern Nigeria during the

381 ascending and maximum phases of solar cycle 24 have been carried out. Our result shows that

382 OBS-TEC and IRI-2016 model rising from a minimum in the early hours of the day to a broad

383 daytime maximum before falling steeply to a minimum after sunset for all years, due to

384 photoionization increase produced by solar extreme ultraviolet (EUV) radiation. ~~Magnetic field~~

385 ~~tubes are rapidly filled up at dawn resulting in the increase of extreme ultraviolet (EUV) ionization~~

386 (Anderson et al., 2004; D'ujanga et al., 2017). The diurnal variation reveals that the peak of OBS-

387 TEC ~~of~~ is often delayed when compared with IRI-2016 model, with the maximum occurring

388 afternoon ~~many of the months were delayed till after-noon~~, showing dome-like shape while noon

389 bite-out, a special feature observed in equatorial/ low latitude is seen in the peak of majority of the

390 plots of IRI-2016 model. On a general note, we concluded that IRI-2016 model cannot be used as

391 proxy for TEC measurements for most hours of the day for the years investigated. Our result agree

392 with those of Komjathy et al. (1998); Lee and Reinisch (2006); Malik et al. (2016); Bhuyan and

393 Borah (2007); Mosert et al. (2007) and Sethi et al. (2010) at their respective locations. For all

394 seasons, pre-midnight (18 – 23 h) values of TEC are higher than post-midnight (00 – 05 h) TEC

395 values during all years. Seasonal variation shows an asymmetry in the equinoxes and solstices in

396 the NEI as also reported by ~~in the research of~~ Fayose et al. (2012) ~~working at Ilorin in the NEI~~ and

397 Eyelade et al. (2017) ~~also working in the NEI~~. Maximum OBS-TEC values in 2011 and 2012 were

398 recorded in September equinox ~~season~~. In 2013, OBS-TEC reached its maximum during the

399 December solstice ~~season~~ while in 2014, the maximum OBS-TEC was recorded in March equinox

400 ~~season~~. This result agrees in general with those of D'ujanga et al. (2017) in the East African sector

401 and Bagiya et al. (2009) in the Indian sector, who obtained higher TEC values during the equinoxes

402 than during the solstices. Thermospheric neutral compositions is a major cause of seasonal

403 variation of ionospheric parameters such as TEC, since during the day the equator is hotter than

404 the poles. Finally, monthly ~~annual~~ OBS-TEC varies linearly with annual sunspot number, Rz, thus

405 revealing strong dependence of TEC on solar activity (sunspot number). This linearity collapsed

406 in the month of July of 2012 and 2014. OBS-TEC and sunspot number were found to increase

407 gradually from 2011 to 2014 in agreement with Rama Rao et al. (1985) showing that there is a

408 direct solar control on TEC.

409 **ACKNOWLEDGEMENT**

410 We thank the Office of the Surveyor General of the Federation (OSGoF-Nigeria) for making TEC

411 data available through the infrastructure www.nignet.net. We also thank Hatanaka, Y., Gopi

412 Krishna for providing TEC processing software online. Finally, we appreciate Bilitza et al. (2017)

413 for making the latest version of IRI model available online.

414 **REFERENCES**

415 Aggarwal, M., Bardhan, A., Sharma, D.K. Equinoctial asymmetry in ionosphere over Indian

416 region during 2006 – 2013 using COSMIC measurements. Advances in Space Res., 60, 999 –

417 1014, 2017.

418 Akala, A.O., Somoye, E.O, Adeloye, A.B., Rabiu, A.B. Ionospheric f_oF_2 variability at equatorial

419 and low latitudes during high, moderate and low solar activity. Indian Journal of Radio and Space

420 Physics.Vol. 40, 124 – 129, 2011.

421 Akala, A.O., Seemala, G.K., Doherty, P.H., Valladares, C.E., Carrano, C.S., Espinoza, J., and

422 Oluyo, K.S. Comparison of equatorial GPS-TEC observations over an African station and an

423 American station during the minimum and ascending phases of solar cycle 24. Ann. Geophys., 31,

424 2085, 2013.

425 Alizadeh, M.M., Wijaya, D.D., Hobiger, T., Weber, R., Schuh, H. Ionospheric effects on

426 microwave signals in J. Bohm and H. Schuh (eds). Atmospheric Effect in Space Geodesy. Springer

427 atmospheric sciences. Doi: 10.1007/978-3-642-36932-2_2, © Springer-Verlag Berlin Heidelberg,

428 2013.

429 Anderson, D., Anghel, A., Chau, J., Veliz, O. Daytime vertical $\mathbf{E} \times \mathbf{B}$ drift velocities inferred from

430 ground-based magnetometer observations at low latitudes, Space Weather, 2, S11001; doi:

431 10.1029/2004SW000095, 2004.

432 Ayorinde, T.T., Rabiu, A.B., and Amory-Mazaudier, C. Inter-hourly variability of Total Electron

433 Content during the quiet condition over Nigeria within the Equatorial Ionization Anomaly region.

434 J. Atmos. Solar Terr. Phys., 145, 21 – 33, 2016.

435 Berkner, L.V. and Wells, H.W. F-region ionosphere – investigation at low latitude. Terres. Magn.,

436 39, 215, 1934.

437 Bagiya, M.S., Joshi, H.P., Iyer, K.N., Aggarwal, M., Ravin-dran, S., and Pathan, B.M. TEC

438 variations during low solar activity period (2005 – 2007) near the Equatorial Ionization Anomaly

439 Crest region in India. Ann Geophys., 27, 1047 – 1057, 2009.

440 Balan, N., Bailey, G.J., Moffett, R.J. Modelling studies of ionospheric variations during an intense

441 solar cycle. J. Geophys. Res., 99, 17467 – 17475, 1994.

442 Balan, N., Bailey, G.J., Su, Y.Z. variations of the ionosphere and related solar fluxes during solar

443 cycle 21 and 22. Advances in Space Res., 18, 11 – 14, 1996

444 Bhuyan, P.K. and Borah, R.R. TEC derived from GPS network in India and comparison with the

445 IRI. Advances in Space Res., 39, 830 – 840, 2007.

446 Bilitza, D., Altadill, D., Zhang, Y., Mertens, C., Truhlik, V., Richards, P., McKinnell, L.A.,

447 Reinisch, B. International reference ionosphere 2012 – A model of international collaboration. J.

448 Space Weather Space Clim., 4, 1 – 12, doi: 10.1002/201JA018009, 2014.

449 Bilitza, D., Altadill, D., Truhlik, V., Shubin, V., Galkin, I., Reinisch, B., and Huang, X.

450 International reference ionosphere 2016: from ionospheric climate to real-time weather

451 predictions. Space weather, 15, 418 – 429, doi: 10.1002/20165SW001593, 2016.

452 Bolaji, O. S., Adeniyi, J.O., Radicella, S.M., and Doherty, P.H. Variability of total electron content

453 over an equatorial West African station during low solar activity. Radio Sci., 47, RS1001, doi:

454 10.1029/2011RS004812, 2012.

455 Charkrabarty, D., Bagiya, M.S., Thampi, S.V., Iyer, K.N. Solar EUV flux (0.1 – 50 nm), $F_{10.7}$ cm

456 flux, sunspot number and total electron content in the crest region of the ionization anomaly during

457 the deep minimum between solar cycle 23 and 24. Indian Radio and Space Phys., 41, 110 – 120,

458 2012.

459 Ciraolo, L., and Spalla, P. TEC analysis of IRI simulated data. Adv. Space Res., 29, 6, 959 – 966,

460 2002.

461 Codrescu, M. V., Palo, S. E., Zhang, X., Fuller-Rowell, T. J., Poppe, C. TEC climatology derived

462 from TOPEX/POSEIDON measurements, Journal of Atmospheric Solution, 61, 281-298, 1999.

463   Dabas, R.S., Singh, L., Lakshmi, D.R., Subramanyam, P., Chopra, P., Garg, S.C. Evolution and

464   dynamics of equatorial plasma bubbles: relationships to $\mathbf{E} \times \mathbf{B}$ drifts, post-sunset total electron

465   content enhancements, and equatorial electrojet strength. Radio Sci., 38, doi:

466   10.1029/2001RS002586, 2003.

467   D'ujanga, F.M., Opio, P. Twinomugisha, F. Variation of total electron content with solar activity

468   during the ascending phase of solar cycle 24 observed at Makerere University, Kampala. Space

469   Weather: Longitude and Hemispheric Dependences and Lower Atmosphere Forcing, Geophysical

470   Monograph 220, First Edition. Edited by Timothy Fuller-Rowell, Endawoke Yizengaw, Patricia

471   H. Doherty, and Sunanda Basu. © 2017 American Geophysical Union. Published 2017 by John

472   Wiley & Sons, Inc., 2017.

473   Eyelade, V.A., Adewale, A.O., Akala, A.O., Bolaji, O.S. and Rabiu, A.B. Studying the variability

474   in the diurnal and seasonal variations in GPS TEC over Nigeria. Ann. Geophys., 35, 701 – 710,

475   2017.

476   Fayose, R.S., Rabiu, B., Oladosu, O., Groves, K. Variation of total electron content (TEC) and

477   their effect on GNSS over Akure. Nigeria, Applied Physics Research, 4, 2, 2012.

478   Forbes, J.M., Bruinsma, S., Lemoine, F.G. Solar rotation effects in the thermospheres of Mars

479   and Earth. Science, 312, 1366–1368, 2006.

480   Gorney, D. J. Solar cycle effects on the near-earth space environment. Rev Geophys, 28, 315–

481   336, 1990.

482   Hajra, R., Chakraborty, S.K., Tsurutani, B.T., DasGupta, A., Echer, E., Brum, C.G.M., Gonzalez,

483   W.D., Sobral, H.A. An empirical model of ionospheric total electron content (TEC) near the crest

484   of the equatorial ionization anomaly (EIA). J. Space Weather Space Clim., 6, A29, doi:

485   10.1051/swsc/2016023, 2016.

486   Jee, G., Schunk, R. W., Scherliess, L. Analysis of TEC data from the TOPEX/Poseidon mission,

487   Journal of Geophysical Research, 109, A01301, doi:10.1029/2003JA010058, 2004.

488   Komjathy, A., Langley, R., Bilitza, D. ingesting GPS-derived data into the IRI for single frequency

489   radar altimeter ionospheric delay corrections. Adv. Space Res., 22, 6, 793 – 802, 1998.

490   Langley, R., Fedrizzi, M., Paula, E., Santos, M., Komjathy, A. Mapping the low latitude

491   ionosphere with GPS. GPS World, 13, 2, 41 – 46, 2002.

492   Lee, C.C. and Reinisch, B.W. Quiet condition hmF2, NmF2 and Bo variations at Jicamarca and

493   comparison with IRI-2001 during solar maximum. J. Atmos. Solar Terr. Phys., 68, 2138 – 2146,

494   2006.

495   Liu, L., Wang, W., Chen, Y., Le, H. Solar activity effects on the ionosphere: A brief review. Space

496   Physics and Space Weather Geophysics. Chinese science Bulletin. 56, 12, 1202 – 1211, 2011.

497   Liu, L., Wang, W., Ning, B., Pirog, O.M., and Kurkin, V.I. Solar activity variations of the

498   ionospheric peak electron density. J. Geophys. Res., vol 111, A08304, doi:

499   10.1029/2006JA011598, 2006

500   Malik, R.A., Abdullah, M., Abdullah, S., Homam, M.J. Comparison of Maximum Useable

501   Frequency (MUF) variability over Peninsular Malaysian with IRI Model during the rise of solar

502   cycle 24. J. Atmos. Solar Terr. Phys., 138 – 139, 87 – 92, 2016.

503

504   Maruyama, T., Ma, G., and Nakamura, M. Signature of TEC storm on 6 November 2001 derived

505   from dense GPS receiver network and ionosonde chain over Japan. Journal of Geophysical

506   Research, 109, A10302, doi: 10.1029/2004JA010451, 2004.

507   Mosert, M., Gende, M., Brunini, C., Ezquer, R. and Altadill, D. Comparisons of IRI TEC with

508   GPS and Digisonde measurements at Ebro. Advances in Space Res., 39, 841 – 847, 2007.

509   Okoh, D., Lee-Anne McKinnell, L., Cilliers, P., Okere, B., Okonkwo, C., Rabiu, A.B. IRI-VTEC

510   versus GPS-vTEC for Nigerian SCINDA GPS stations. Advances in Space Research,

511   http://dx.doi.org/10.1016/j.asr.2014.06.037, 2014.

512   Ogunmodimu, O., Rogers, N.C., Falayi, E., Bolaji, S. Solar Flare induced cosmic noise absorption,

513   NRIAG Journal of Astronomy and Geophysics. 7, 1, 31-39, 2018.

514   Ogwala, A., Somoye, E.O., Oyedokun, O., Adeniji-Adele, R.A., Onori, E.O., Ogungbe, A.S.,

515   Ogabi, C.O., Adejo, O., Oluyo, K.S., Sode, A.T. Analyses of Total Electron Content over Northern

516   and Southern Nigeria. J. Res. and Review in Sci., 21 – 27, 2018.

517   Onwumechilli, C.A., and Ogbuehi, P.O. Journal Atmos. Terr. Phys., 26, 894, 1964.

518   Rama Rao, P.V.S., Niranjan, K., Rama Rao, B.V., Rama Rao, B.V.P.S., Prasad, D.S.V.V.D. Proc.

519   URSI/ IPS Conference on the ionosphere and Radio wave Propagation. Sydney, Australia, 1985.

520   Rama Rao, P.V.S., Krishna, S.G., Prasad, J.V., Prasad, S.N.V.S., Prasad, D.S.V.V.D., Niranjan,

521   K. Geomagnetic storm effects on GPS based navigation. Ann. Geophys., 27, 2101 – 2110, 2009.

522   Rama Rao, P.V.S., Krishna, S.G., Niranjan, K., Prasad, D.S.V.V.D. Study of temporal and spatial

523   characteristics of L-band scintillation over the Indian low-latitude region and their possible effects

524   on GPS navigation. Ann. Geophys., 24, 1567 – 1580, 2006a.

525   Rama Rao, P.V.S., Krishna, S.G.,Niranjan, K., Prasad, D.S.V.V.D. Temporal and spatial

526   variations in TEC using simultaneous measurements from indian GPS network of receivers during

527   low solar activity period of 2004 – 2005. Ann. Geophys., 24, 3279 – 3292, 2006b.

528   Rama Rao, P.V.S., Niranjan, K., Prasad, D.S.V.V.D., Krishna, S.G., Uma, G. On the validity of

529   the ionospheric pierce point (IPP) altitude of 350km in the Indian equatorial and low-latitude

530   sector. Ann. Geophys., 24, 2159 – 2168, 2006c.

531   Sethi, N. K., Pandey, V. K., Mahajan, K. K. Comparative study of TEC with IRI model for solar

532   minimum period at low latitude. Advances in Space Research, 27, 45 – 48, 2010.

533   Suranya, P.L., Prasad, D.S.V.V.D., Niranjan, K., Rama Rao, P.S.V. Short term variability in foF2

534   and TEC over low latitude stations in the Indian sector. Indian J. of Radio and Space Phys., 44, 14

535   – 27, 2015.

536   Somoye, E.O. Diurnal and seasonal variation of fading rates of E- and F-region echoes during IGY

537   and IQSY at the equatorial station of Ibadan. Indian Journal of Radio and space Physics, 38, 194

538   – 202, 2010.

539   Somoye, E.O., Akala, A.O., Ogwala, A. Day-to-day variability of h'F and foF2 during some solar

540   cycle epochs. Journal Atmos. Solar Terr. Physics, 73, 1915 – 1922, 2011.

541   Stankov, S. M. Trans-ionospheric GPS signal delay gradients observed over mid-latitude Europe.

542   Advances in Space Research, 43, 1314–1324, 2009.

543   Sunda, S. and Vyas, B.M. Local time, seasonal and solar cycle dependency of longitudinal

544   variations of TEC along the crest of EIA over India. J. Geophys. Res., vol 118, 6777 – 6785, 2013.

545 Tariku, Y.A. Pattern of GPS-TEC variability over low-latitude regions (African sector) during the

546 deep solar minimum (2008 to 2009) and solar maximum (2012 to 2013) phases. Earth, Planets,

547 and space. 67, 35, 2015.

548 Titheridge, J.E. Changes in atmospheric composition inferred from ionospheric production rates.

549 J. Atmos. Terr. Phys., 36, 1249 – 1257, 1974.

550 Torr, M.R. and Torr, D.G. The seasonal behavior of the F2 layer of the ionosphere. J. Atmos. Terr.

551 Phys., 35, 2237, 1973.

552 Tsai Ho-Fang, Liu Jann-Yenq, Tsai Wei-Hsiung and Liu Chao-Han, Tseng Ching-Liang and Wu

553 Chin-Chun. Seasonal variations of the ionospheric TEC in Asian equatorial anomaly regions. J.

554 Geophysical Res., vol 106, A12, 30,363 – 369, 2001.

555 Wanninger, L. Effects of the equatorial ionosphere on GPS. GPS World, 2, 48, 1993.

556 Wu, C.C., Liou, K., Shan, S.J., Tseng, C.L. Variation of ionospheric total electron content in

557 Taiwan region of the equatorial anomaly from 1994 – 2003. Adv. Space Res., 41, 611 – 616, 2008.

558